PERFORMANCE AND ECONOMIC EVALUATION OF SOLAR HEATING AND COOLING SYSTEMS AT DIFFERENT LOCALITIES IN EGYPT (THEORETICAL STUDY)

A.A. Ghoneim
Math. & Eng. Physics Dept., Faculty of Engineering,
Alex. University, Alexandria, Egypt

and M.M. Sorour
Mechanical Eng. Dept., Faculty of Engineering,
Alex. University, Alexandria, Egypt

ABSTRACT

In this investigation, the performance and economic evaluation of a solar heating and cooling system are studied using the transient simulation program (TRNSYS). The water heating load, space heating load, and the cooling load of a typical Egyptian house were considered. The study involves five different localities which were chosen to represent the climatic changes all over Egypt. These localities are : Aswan (Upper Egypt), Kharga (Western Desert), Asyout(Middle Egypt), Cairo (Cairo), and Marsa Matrouh (Mediterranean). The results showed that the optimum solar collector areas vary significantly with localities in Egypt and using evacuated tube collectors significantly reduces the optimum area but not the cost of energy unit. Also, in all localities, great portion of the total load is covered by solar energy. In addition, the cost of energy unit for solar heating and cooling system was found to be varied from 68 to 83% of the corresponding cost of the conventional fuel at the current prices. However, with addition of insulation for the building, the cost of the solar system decreases which is more feasible in all localities.

Keywords: Solar heating and cooling systems, Heating load, Cooling load, Solar fraction, Absorption chiller, Coefficient of performance, Collector efficiency, Life cycle savings of a solar system, Economic analysis.

Nomenclature

- A_c collector area (m^2)
- A_s storage tank surface area (m^2)
- c_p specific heat of the water (J/kg K)
- C_A solar energy investment cost which is directly proportional to collector area ($)
- C_E solar energy investment cost which is independent of collector area ($)
- C_F unit cost of delivered conventional energy for the first year of analysis ($)
- F_{AC} solar fraction of space cooling
- F_D solar fraction of domestic water heating
- F_s solar fraction of space heating
- F_t total solar fraction
- F_R heat removal factor
- G incident radiation on horizontal surface (W/m2)
- K_T clearness index
- L total load (kJ)
- L_{CS} life cycle savings ($)
- M_s mass of the water in the storage tank (kg)
- P_1 factor relating life cycle fuel cost to first year fuel cost savings
- P_2 factor relating life cycle by additional capital investment to initial investment
- Q_u useful energy rate gained by the collector (W)
- T_a ambient temperature (°C)
- t time (s)
- T_i inlet collector temperature (°C)
- T_o outlet collector temperature (°C)
- T_{RN} temperature of the combined stream of water returning from the air conditioner or air heater, and service hot water systems (°C)
- T_s temperature of the water in the energy

storage tank (°C)
U_L collector overall heat transfer loss coefficient (W/m^2 K)
U_{Ls} storage tank heat transfer loss coefficient (W/m^2 K)
m_c mass flow rate of water to the collector (kg/s)
m_F mass flow rate of water to the air conditioner or air heater (kg/s)
m_L mass flow rate of water to the service hot water system (kg/s)
W_s wind speed (m/s)
η_{AC} space cooling efficiency
η_c collector efficiency
η_D domestic water heating efficiency
η_s space heating efficiency
η_t total system efficiency
$(\tau\alpha)$ transmittance-absorptance product

I-INTRODUCTION

Active solar heating systems are now widely used in many applications, while, active solar cooling systems are not. Numerous publications investigated the performance of the solar heating systems [1,2,3]. On the other hand, there are much fewer publications discussing the performance of solar cooling and air conditioning systems.

Van Hattem and Dato [4] had conducted an experimental study of a solar powered cooling system in Ispra, Italy. The overall cooling efficiency (the ratio of cooling load to total solar energy) was found to be around 11%. In saudi Arabia, a 3.5 ton LiBr absorption chiller system with flat plate collectors was installed and tested by Sayigh and Khoshaim [5]. In Singapore, a 7 kW solar cooling system was built and the solar cooling efficiency was found to be approximately equal to 10%. Yeung et al [6] studied the feasibility of utilizing solar energy for comfort cooling in Hong Kong. They constructed a solar energy absorption air conditioning system on the campus of the University of Hong Kong. The system had an overall efficiency of approximately 8% and an average solar fraction of 55%. Lof et al. [7] made an extensive study of solar heating and cooling systems for eight cities in the U.S.A. The system has been optimized to minimize the annual energy cost. Nakahara et al. [8] studied the performance of a solar heating and cooling system. Their results showed that the system was able to provide all the required heating energy in the winter and 70% of the energy needed to drive the absorption chiller on a typical summer day.

The purpose of the present study is to investigate theoretically the feasibility and the operation of a solar system designed for space heating, domestic water heating, and cooling requirements of a standard house in Egypt. The performance of the solar system is studied at five different localities in Egypt. These localities represent diverse Egyptian climatic conditions. The localities studied are Aswan (Upper Egypt, Latitude 24°), Kharga (Western Desert, Latitude 25.5°), Asyout (Middle Egypt, Latitude 27°, Cairo (Cairo, Latitude 30°), and Marsa Matrouh (Mediterranean, latitude 31.30°).

The transient simulation program (TRNSYS) developed by Klein et al. [9] is used to determine the solar fraction of the proposed system. On the other hand, the economic calculations for this study are based on life cycle savings (LCS) method developed by Brandemuhel et al. [10].

II- SYSTEM DESCRIPTION AND CONTROL STRATEGY

Figure (1) shows a schematic representation of the system used. The main system components are a flat plate collector, a storage tank, an absorption chiller, heat exchanger, and auxiliary units.

There are four different modes for the system operation. When solar energy is available for collection and there is a load demand, heat is supplied directly from the collector to the heating or cooling unit. When solar energy is available for collection and there is no heat or cooling demand, heat is stored in the storage unit. On the other hand, if solar energy is not available for collection and there is a load demand, storage then supplies heat to the heating or cooling unit. However, if storage temperature is not sufficient, the heating or cooling load is supplied by the auxiliary source.

Figure (2) shows a schematic of a single lithium bromide water absorption chiller. The hot water, chilled water and condensing water loops are clearly presented in the diagram. The chiller model is based on a commercially available lithium bromide-water absorption chiller, Arkla model WF-36. The Arkla chiller has a nominal cooling capacity of three tons (37980 kJ/h). Units of different capacity are approximated by scaling the Arkla performance.

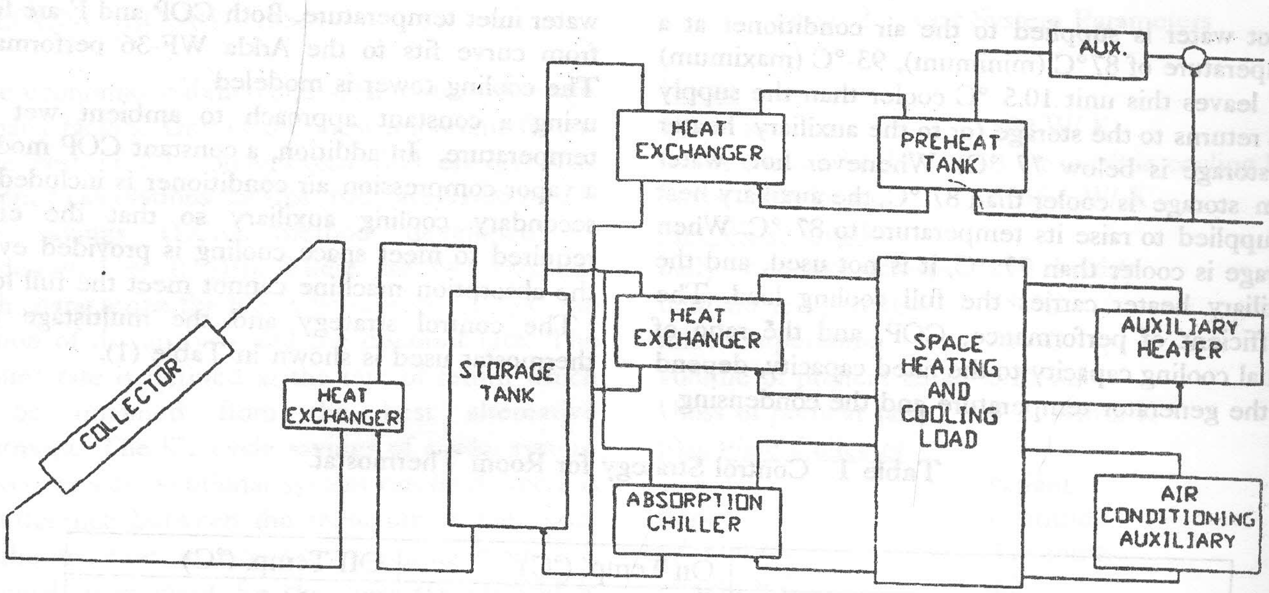

Figure 1. Schematic diagram of the solar system.

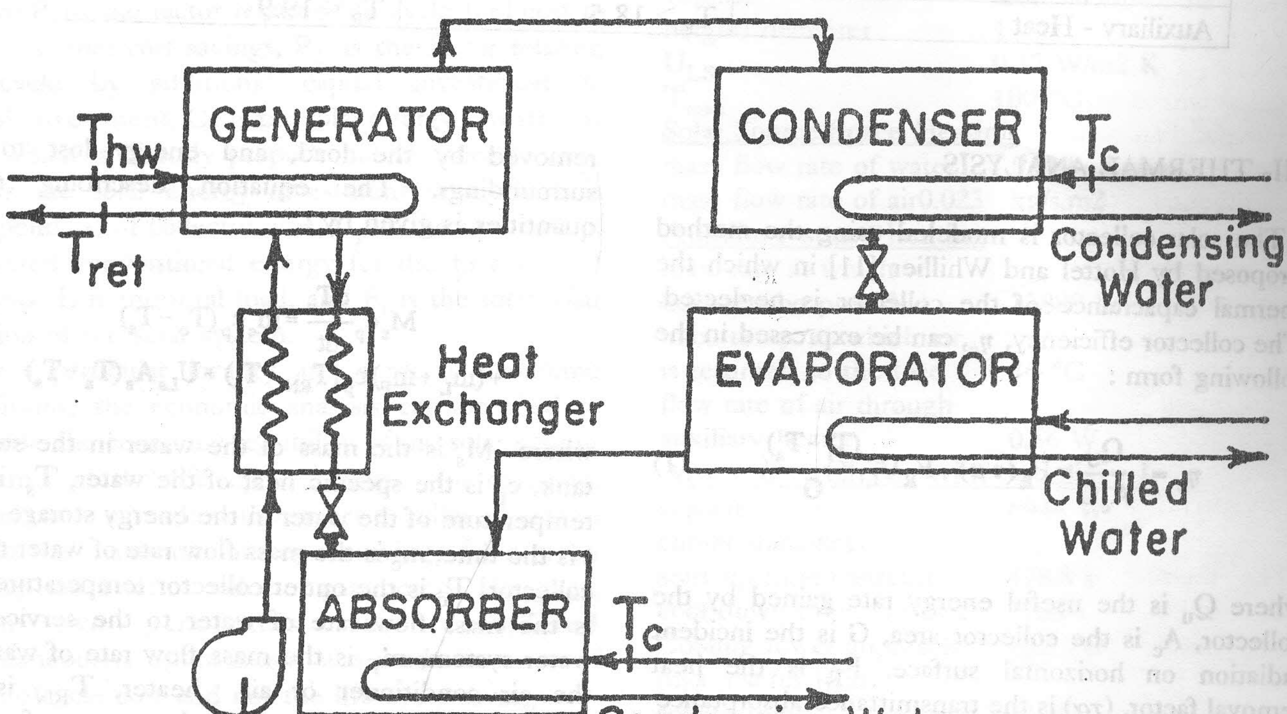

Figure 2. Single effect absorption chiller.

Hot water is supplied to the air conditioner at a temperature of 87°C (minimum), 93 °C (maximum) and leaves this unit 10.5 °C cooler than the supply and returns to the storage (or to the auxiliary heater if storage is below 77 °C). Whenever hot water from storage is cooler than 87 °C, the auxiliary heat is supplied to raise its temperature to 87 °C. When storage is cooler than 77 °C, it is not used, and the auxiliary heater carries the full cooling load. The coefficient of performance, COP, and the ratio of actual cooling capacity to the rated capacity, depend on the generator temperature and the condensing water inlet temperature. Both COP and F are found from curve fits to the Arkla WF-36 performance. The cooling tower is modeled using a constant approach to ambient wet bulb temperature. In addition, a constant COP model of a vapor compression air conditioner is included as a secondary cooling auxiliary so that the energy required to meet space cooling is provided even if the absorption machine cannot meet the full load.

The control strategy and the multistage room thermostat used is shown in Table (1).

Table 1. Control Strategy for Room Thermostat.

	On Temp. (°C)	Off Temp. (°C)
Solar- AC	$T_R > 24.9$	$T_R < 24.3$
Auxiliary I- AC	$T_R > 25.6$	$T_R < 25.0$
Auxiliary II-AC	$T_R > 26.7$	$T_R < 26.1$
Solar- Heat	$T_R > 20.0$	$T_R < 21.5$
Auxiliary - Heat	$T_R > 18.5$	$T_R < 19.9$

III- THERMAL ANALYSIS

The solar collector is modeled using the method proposed by Hottel and Whillier [11] in which the thermal capacitance of the collector is neglected. The collector efficiency, η_c, can be expressed in the following form :

$$\eta_c = \frac{Q_U}{A_c G} = F_R(\tau\alpha) - F_R U_L \frac{(T_i - T_a)}{G} \tag{1}$$

where Q_u is the useful energy rate gained by the collector, A_c is the collector area, G is the incident radiation on horizontal surface, F_R is the heat removal factor, $(\tau\alpha)$ is the transmittance-absorptance product, U_L is the collector overall heat transfer loss coefficient, T_i is the inlet collector temperature, and T_a is the ambient temperature.

The storage tank is modeled as a stratified tank. The energy balance of the water in the storage tank accounts for energy gain from the collector, energy removed by the load, and energy lost to the surroundings. The equation describing these quantities is given by :

$$M_s c_p \frac{dT_s}{dt} = m_c c_p (T_o - T_s) + (m_L + m_F) c_p (T_{RN} - T_s) + U_{Ls} A_s (T_a - T_s) \tag{2}$$

where M_s is the mass of the water in the storage tank, c_p is the specific heat of the water, T_s is the temperature of the water in the energy storage tank, t is the time, m_c is the mass flow rate of water to the collector, T_o is the outlet collector temperature, m_L is the mass flow rate of water to the service hot water system, m_F is the mass flow rate of water to the air conditioner or air heater, T_{RN} is the temperature of the combined stream of water returning from the air conditioner or air heater, and service hot water systems, U_{Ls} is the storage tank heat transfer loss coefficient, and A_s is the storage tank surface area.

IV- ECONOMIC ANALYSIS

The economic viability of a solar system depends on many factors. One of the most important factors is the cost of the conventional fuel energy. The economic calculations for this study are based on life cycle savings (LCS) method developed by Brandemuhel et al. [10]. There are two variables which characterize the life cycle savings method: the duration of the analysis and the discount rate. The discount rate is defined as the rate of return which can be obtained from the best alternative investment. The life cycle savings of a solar system (LCS) over a conventional system can be defined as the difference between the reduction in fuel costs and the increase in expenses resulting from the additional investment for the solar system and is given by the following equation :

$$LCS = P_1 C_F LF_t - P_2 (C_A A_c + C_E) \qquad (3)$$

where P_1 is the factor relating life cycle fuel cost to first year fuel cost savings, P_2 is the factor relating life cycle by additional capital investment to initial investment, C_A is the solar energy investment cost which is directly proportional to collector area, C_E is the solar energy investment cost which is independent of collector area, C_F is the unit cost of delivered conventional energy for the first year of analysis, L is the total load, and F_t is the total solar fraction of the solar system.

For a particular locality and a set of economic conditions, the economic analysis can be used to evaluate the economic feasibility of the solar system in terms of the life cycle savings. For example, optimization is made with respect to collector area to obtain the maximum life cycle savings for a given locality and a set of collector parameters. However, when two parameters were considered simultaneously, optimization was made in terms of the life cycle cost and not the life cycle savings.

V- SYSTEM PARAMETERS AND DATA

Table (2) shows the system parameters for the different components of the system studied.

Table 2. Solar System Parameters

House	
UA house	500 W/ K
latent cooling load	0.3 x sensible cooling load
house capacitance	5555.6 W/ K
Hot Water Load	
daily hot water demand	250 kg/day
demand temperature	55 °C
inlet temperature	20 °C
volume of preheat tank	0.25 m3
Uloss of preheat tank	0.47 W/m2 K
Flat Plate Collector	
area	variant
slope	= latitude
orientation	due south
ground reflectance	0.2
$F_R (\tau\alpha)$	0.7
$F_R U_L$	6 W/m2 K
mass flow rate	0.014 kg/s.m2
Storage Tank	
volume	0.08 m3/m2
height/ diameter	1
U_{LS}	0.47 W/m2 K
T_{max}	100 °C
Solar Source Space Heating	
mass flow rate of water	0.014 kg/s.m2
mass flow rate of air	0.023 kg/s.m2
Auxiliary space heating	
max. rate at which heat can be provided	13889 W
max. temp. at which air is returned to the load	46 °C
flow rate of air through auxiliary heater	0.56 W
Absorption Chiller with Auxiliary I	
capacity	6944 W
chiller transients	
start up time constant	478.8 s
cool down time constant	3780 s
Cooling tower approach	10.5 °C
max. useful solar source temp	77 oC
Auxiliary energy to generator	
temp. of firing water delivered	93 °C
series auxiliary if solar source temp.	> 87 °C

parallel auxiliary if solar source temp.	< 87 °C
Air Conditioner Auxiliary II	
capacity	6944 kJ/h
COP	2.0
Economic Parameters	
cost per unit area (FPC)	200 $/m2
cost per unit area (ETC)	400 $/m2
area independent cost	2000 $
cost of conventional fuel in 1st year	0.0324 $/kW.hr
annual increase in fuel cost	5%
% extra insurance and maintenance in year 1	2%
term of mortage	20 years
period of economic analysis	20 years

Table (3) shows the monthly weather data for one of the selected localities (Aswan). The data file of each locality contains monthly average values of daily radiation on a horizontal surface in kWh/m^2/day (G), clearness index (K_T), maximum air temperature in degrees Celsius (T_{max}), minimum air temperature in degrees Celsius (T_{min}), relative humidity in percentage (R.H), and wind speed in km/hour (w_s). These data were provided by the National Geophysics Institute at Cairo, Egypt.

Table 3. Monthly Weather Data for Aswan, Egypt.

Month	G	T_{min}	T_{max}	R.H	K_T	w_s
Jan.	4.70	8.1	23.5	35	0.72	8.0
Feb.	5.65	9.6	26.2	26	0.73	8.4
Mar.	6.61	13.0	30.5	18	0.73	9.1
Apr.	7.41	17.9	35.3	14	0.74	9.3
May	7.68	21.4	38.7	13	0.75	8.8
Jun.	8.02	24.3	41.8	13	0.76	9.0
Jul.	7.94	24.8	41.1	16	0.77	8.2
Aug.	7.45	24.8	41.0	18	0.74	8.2
Sep.	6.76	22.6	39.5	20	0.72	8.5
Oct.	5.81	19.6	36.4	22	0.70	8.2
Nov.	7.96	14.6	29.8	33	0.68	8.1
Dec.	4.39	9.7	25.0	37	0.66	7.8

VI- RESULTS AND DISCUSSION

The thermal and economic characteristics are presented in the following section for Cairo as a representative sample for the different localities. The plot in Figure (3) shows the variation of the solar fraction of space heating (F_S), domestic water heating (F_D), and cooling load (F_{AC}) as well as the total fraction (F_t) with collector area. As seen from the figure, the solar fraction for space heating and domestic water heating are nearly satisfied at areas around 30 m^2. Conversely, the space cooling require much greater areas.

The variation of total solar fraction, life cycle savings, and overall system efficiency (ratio of solar energy provided to the system to the total incident radiation) with collector area is presented in Figure (4). This typical figure shows the choice of optimum collector area which is equal to 28 m^2 in this case. It is clear from this figure that this optimum area neither corresponds to maximum system efficiency nor to the maximum solar fraction.

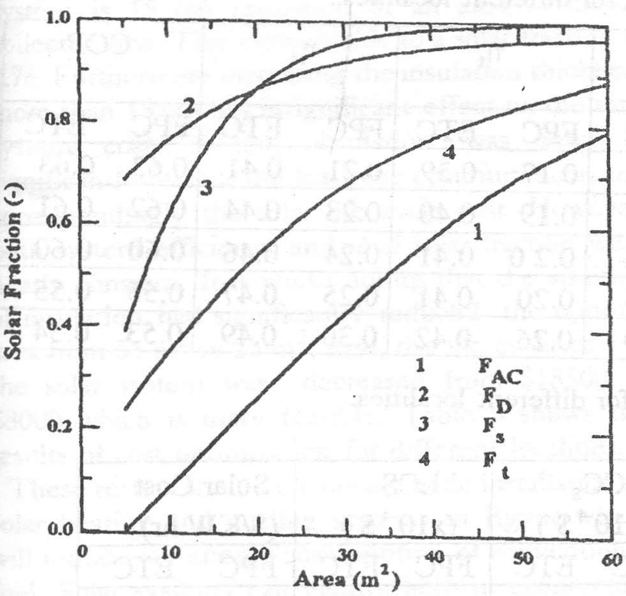

Figure 3. Variation of solar fraction with collector area for Cairo, Egypt (FPC).

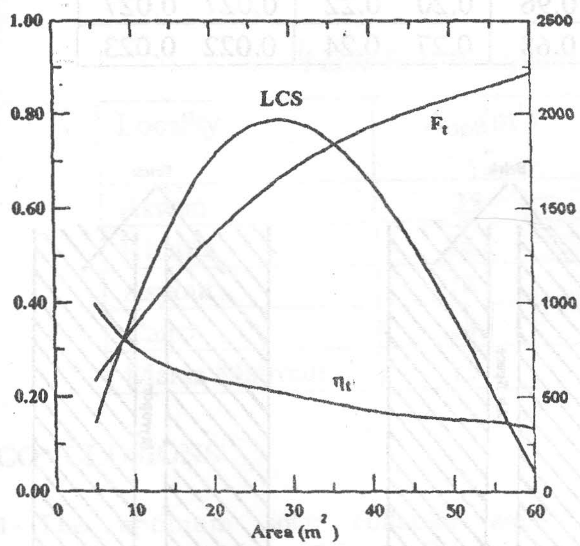

Figure 4. Solar system characteristics for Cairo.

Figure (5) shows the variation of space heating efficiency , domestic water heating efficiency, space cooling efficiency, and the total system efficiency, through the year for the optimum area for Cairo. As expected, the efficiency of the space heating and the space cooling diminishes during the summer and winter seasons respectively, while the domestic hot water efficiency remains approximately constant. It is to be noted that when the coefficient of performance (COP) was calculated for this example an average value of 0.55 was assessed for the seven months of operation.

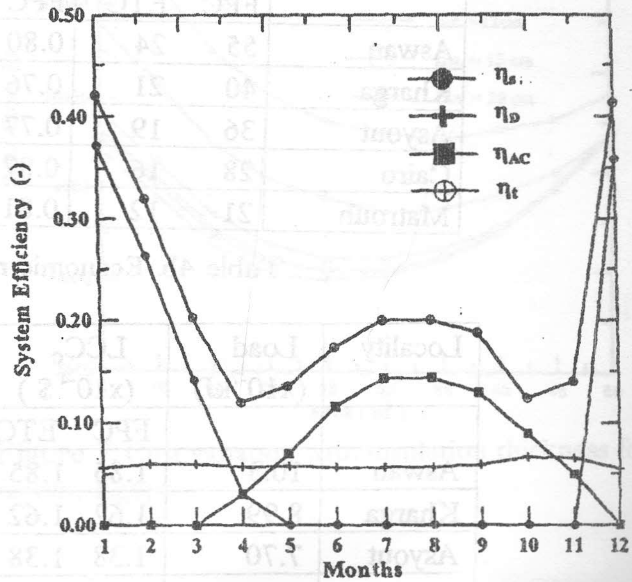

Figure 5. Variation of system efficiency through the year for Cairo.

The previous results are obtained with a flat plate collector (FPC) with a value of FR $(\tau\alpha)$ equal to 0.7, and $F_R U_L$ value equal to 6 W/m^2. To investigate the feasibility of the evacuated tube collectors (ETC), this study was repeated using values of $F_R(\tau\alpha)$ equal to 0.85, and $F_R U_L$ value equal to 2.5W/m^2.

Table (4a) presents the performance results of different localities. It can be seen that the optimum area varies significantly with latitude, and this optimum areas using ETC are nearly half that of FPC. In addition, the total solar fraction (F_t) for FPC and ETC are nearly equal for all localities and satisfy accepted portions of the load. On the other hand, the efficiency of the system (η_t) increases steadily as going from hot severe weather conditions (Aswan) to moderate weather conditions (Matrouh) and the effect of ETC on (η_t) is very pronounced. The collector efficiency (η_c) behaves as the system efficiency with slightly higher numerical values. Finally, the coefficient of performance (COP) of the absorption chiller is within the accepted practical values of the conventional lithium bromide system.

Table 4a. Performance results for different localities.

Locality	A_{OP} (m^2)		F_t		η_t		η_c		COP	
	FPC	ETC	FPC	ETC	FPC	ETC	FPC	ETC	FPC	ETC
Aswan	55	24	0.80	0.79	0.17	0.39	0.21	0.41	0.63	0.63
Kharga	40	21	0.76	0.75	0.19	0.40	0.23	0.44	0.62	0.61
Asyout	36	19	0.77	0.76	0.2 0	0.41	0.24	0.46	0.60	0.60
Cairo	28	16	0.87	0.85	0.20	0.41	0.25	0.47	0.55	0.55
Matrouh	21	12	0.81	0.79	0.26	0.42	0.30	0.49	0.53	0.54

Table 4b. Economic results for different localities.

Locality	Load ($x10^{-7}$kJ)	LCC_C ($x10^{-4}$ \$)		LCC_S ($x10^{-4}$ \$)		LCS ($x10^{-4}$ \$)		Solar Cost (\$/KW.hr)	
		FPC	ETC	FPC	ETC	FPC	ETC	FPC	ETC
Aswan	10.3	1.85	1.85	1.29	1.29	0.56	0.56	0.023	0.023
Kharga	8.99	1.62	1.62	1.14	1.16	0.48	0.46	0.023	0.023
Asyout	7.70	1.38	1.38	1.01	1.00	0.37	0.38	0.023	0.023
Cairo	6.53	1.18	1.18	0.98	0.96	0.20	0.22	0.027	0.027
Matrouh	5.27	0.94	0.94	0.65	0.68	0.27	0.24	0.022	0.023

Table (4b) presents the economic results of the system for different localities. The results show the feasibility of the solar system in all localities as indicated by the life cycle savings. The life cycle cost of the conventional and the solar system varies significantly from one locality to another due to the corresponding variation of the total load. However, the cost of 1 kW.hr provided by the proposed solar system is nearly the same for all localities and it is smaller than the value of 0.0324 \$/kW.hr provided by the conventional system.

The feasibility of insulating the house for the purpose of solar heating, and cooling was investigated by assuming that the brick walls have either an additional air space or have an insulation of polystyrene containing an expanding agent (Styropor P 101) of variable thicknesses as shown in Figure (6). In this case, the life cycle savings is not the main parameter since the total system cost depends on two variables mainly, the collector area and the insulation cost. Therefore, the total annual cost of energy is taken as the goal to optimize.

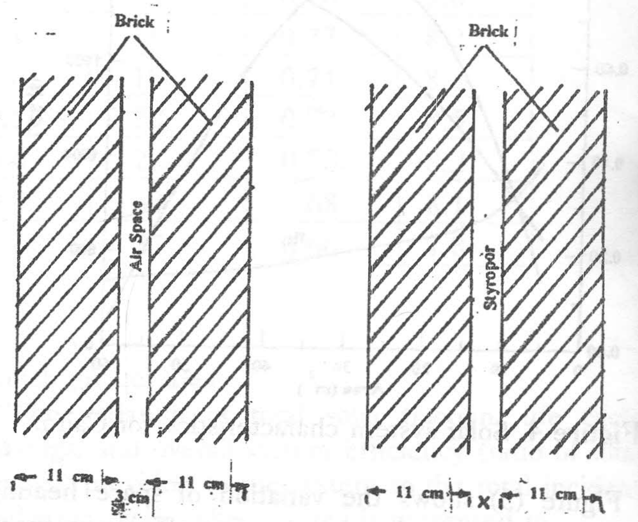

Figure 6. Different house walls configuration.

Figure (7) shows the variation of the total annual cost with area for different wall configurations for Aswan as a sample of the different localities. It can be seen that the optimum configuration of the system is 15 cm insulation at an area of 25 m^2 collector area. This corresponds to a solar fraction of 0.76. Furthermore increasing the insulation thickness more than 15 cm has insignificant effect on the total system cost. Adding insulation was seen to significantly reduce the load, the optimum area, and correspondingly the solar life cycle cost. However, both system efficiency and total solar fraction were nearly constant. It is worth noting that the addition of insulation had significantly reduced the optimal area from 55 m^2 to 25 m^2. Also, the life cycle cost of the solar system was decreased from $18500 to $8000 which is more feasible. Table 5 shows the results of cost optimization for different localities.

These results should encourage wide installation of solar heating and cooling systems in Egypt which will reduce our energy consumption of conventional fuel. Solar systems can greatly help in economical development programs. In addition, wide utilization of solar energy systems, will help in reducing environmental pollution.

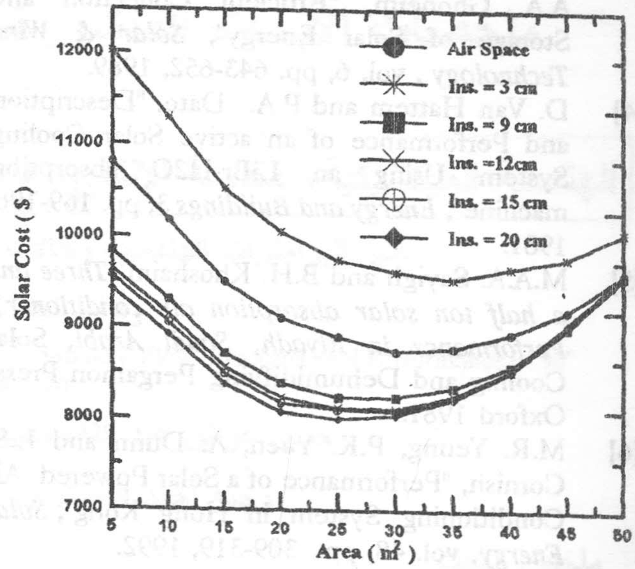

Figure 7. Cost variation with insulation thickness for Aswan, Egypt.

Table 5. Cost Optimization Results for Different Localities.

Locality	$A_{opt}(m^2)$	F_t	Insulation Thick. (cm)	LCC_s ($x10^{-4}$ \$)
Aswan	25	0.76	15	0.80
Kharga	18	0.71	12	0.73
Asyout	16	0.72	10	0.66
Cairo	14	0.65	8	0.59
Marsa Matrouh	11	0.77	5	0.47

CONCLUSIONS

1- The optimum solar collector areas varies significantly with localities in Egypt.

2- Using evacuated tube collectors reduces significantly the optimum area but not the cost of unit energy.

3- In all localities, great portion of the total load is satisfied by solar energy at the optimum conditions and the overall system efficiency is within the previously published results.

4- The cost of unit energy for solar heating and cooling varies from 68% to 83% of the corresponding cost of the conventional fuel at the current prices. However, with addition of insulation of the building, the cost of the solar system decreases which is more feasible in all localities.

REFERENCES

[1] J.A. Duffie and W.A. Beckman, *Solar Engineering of Thermal Processes*, Wiley Interscience , New York, 1980.

[2] H.P. Garg, *Advances in Solar Energy Technology*, D. Reidel Publishing Company, Holland , 1987.

[3] A.S.A. Ammar, A.M. Okaz, M.A. Sorour, and

system is 15 cm insulation at an area of 25 m^2 collector area. This corresponds to a solar fraction of 0.76. Furthermore increasing the insulation thickness more than 15 cm has insignificant effect on the total system cost. Adding insulation was seen to significantly reduce the load, the optimum area, and correspondingly the solar life cycle cost. However, both system efficiency and total solar fraction were nearly constant. It is worth noting that the addition of insulation had significantly reduced the optimal area from 55 m^2 to 25 m^2. Also, the life cycle cost of the solar system was decreased from $18500 to $8000 which is more feasible. Table 5 shows the results of cost optimization for different localities.

These results should encourage wide installation of solar heating and cooling systems in Egypt which will reduce our energy consumption of conventional fuel. Solar systems can greatly help in economical development programs. In addition, wide utilization of solar energy systems, will help in reducing environmental pollution.

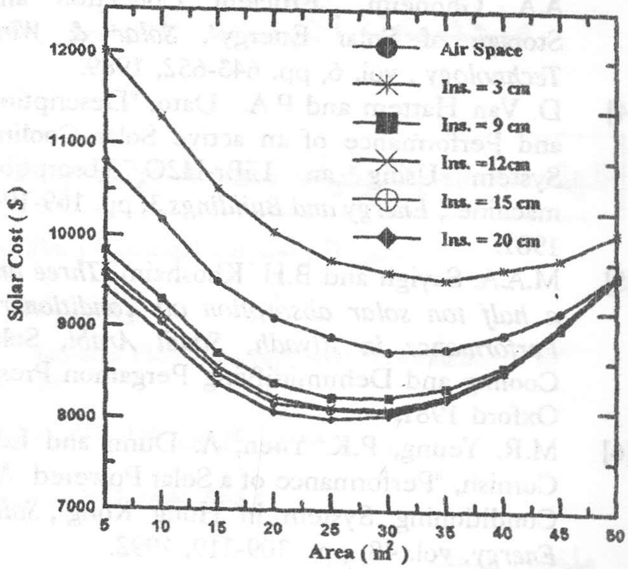

Figure 7. Cost variation with insulation thickness for Aswan, Egypt.

Table 5. Cost Optimization Results for Different Localities.

Locality	$A_{opt}(m^2)$	F_t	Insulation Thick. (cm)	LCC_S ($x10^{-4}$ $)
Aswan	25	0.76	15	0.80
Kharga	18	0.71	12	0.73
Asyout	16	0.72	10	0.66
Cairo	14	0.65	8	0.59
Marsa Matrouh	11	0.77	5	0.47

CONCLUSIONS

1- The optimum solar collector areas varies significantly with localities in Egypt.
2- Using evacuated tube collectors reduces significantly the optimum area but not the cost of unit energy.
3- In all localities, great portion of the total load is satisfied by solar energy at the optimum conditions and the overall system efficiency is within the previously published results.
4- The cost of unit energy for solar heating and cooling varies from 68% to 83% of the corresponding cost of the conventional fuel at the current prices. However, with addition of insulation of the building, the cost of the solar system decreases which is more feasible in all localities.

REFERENCES

[1] J.A. Duffie and W.A. Beckman, *Solar Engineering of Thermal Processes*, Wiley Interscience , New York, 1980.

[2] H.P. Garg, *Advances in Solar Energy Technology*, D. Reidel Publishing Company, Holland , 1987.

[3] A.S.A. Ammar, A.M. Okaz, M.A. Sorour, and

A.A. Ghoneim, "Efficient Collection and Storage of Solar Energy", *Solar & Wind Technology* , vol. 6, pp. 643-652, 1989.

[4] D. Van Hattem and P.A. Dato, "Description and Performance of an active Solar Cooling System Using an LiBr-H2O absorption machine", *Energy and Buildings* 3, pp. 169-196, 1981.

[5] M.A.A. Sayigh and B.H. Khoshaim, *Three and a half ton solar absorption air conditioner's Performance in Riyadh, Saudi Arabi*, Solar Cooling and Dehumidifying Pergamon Press, Oxford 1981.

[6] M.R. Yeung, P.K. Yuen, A. Dunn and L.S. Cornish, "Performance of a Solar Powered Air Conditioning System in Hong Kong", *Solar Energy*, vol. 48, pp. 309-319, 1992.

[7] G.O.G.Lof and R.A. Tybout, "The design and Cost of Optimized Systems for Residential Heating and Cooling by Solar Energy", *Solar Energy*, vol. 16, pp. 9-18 , 1974.

[8] N. Nakahara, Y. Miyakwa and M. Yamamoto, "Experimental Study on House Cooling and Heating with Solar Energy using Flat Plate Collector, *Solar Energy*, vol. 19, pp. 657-662, 1977.

[9] S.A. Klein, et al., "TRNSYS, A Transient Simulation Program", University of Wisconsin-Madison, version 13.1, 1993.

[10] M.J. Brandemuehl and W.A. Beckman, "Economic Evaluation and Optimization of Solar Heating Systems", *Solar Energy*, vol.23, pp. 1-10, 1979.

[11] H.C. Hottel and A. Whillier, Transactions of the Conference on the Use of Solar Energy, 2, Part I, 74, University of Arizona Press, 1958.